Crystal structure of raltegravir potassium, $C_{20}H_{20}FKN_6O_5$

James A. Kaduk,[1,a] Kai Zhong,[2] Amy M. Gindhart,[2] and Thomas N. Blanton[2]
[1]*Illinois Institute of Technology, 3101 S. Dearborn St., Chicago, Illinois 60616*
[2]*ICDD, 12 Campus Blvd., Newtown Square, Pennsylvania 19073-3273*

(Received 9 March 2015; accepted 10 May 2015)

The crystal structure of the potassium salt of raltegravir has been solved and refined using synchrotron X-ray powder diffraction data, and optimized using density functional techniques. Raltegravir potassium crystallizes in space group $P2_1/c$ (#14) with $a = 15.610\ 59(9)$, $b = 8.148\ 19(3)$, $c = 16.125\ 97(6)$ Å, $\beta = 94.1848(5)°$, $V = 2045.72(1)$ Å^3, and $Z = 4$. The most prominent feature of the crystal structure is the chains of edge-sharing 7-coordinate KO_5N_2 parallel to the *b*-axis. The crystal structure can be described as having K-containing layers in the *bc*-plane, with double layers of CH_4F halfway between them. The raltegravir anion is not in the minimum-energy conformation, suggesting that coordination to the K and hydrogen bonds play a significant role in the solid-state structure. The powder pattern is included in the Powder Diffraction File™ as entry 00-064-1499. © *2015 International Centre for Diffraction Data.*
[doi:10.1017/S0885715615000470]

Key words: raltegravir, Isentress®, powder diffraction, Rietveld refinement, density functional theory

I. INTRODUCTION

Raltegravir potassium (marketed as Isentress®) was approved by the U.S. Food and Drug Administration on 12 October 2007 for the treatment of human immunodeficiency virus (HIV) infection. It belongs to the integrase inhibitors class of drugs, working by inhibiting an HIV enzyme integrase that is responsible for the insertion of viral complimentary DNA into the host genome during the pathogenesis of HIV (Croxtall and Keam, 2009). Patent publications WO2010/140156 (Parthasaradhi *et al.*, 2010) and WO2011/024192 (Jetti *et al.*, 2011) described the production of different polymorphs of raltegravir potassium, including amorphous and crystalline forms I, II, III, and H1, but their crystal structures have not been reported. The systematic name (CAS registry number 871038-72-1) is potassium 4-[(4-fluorophenyl)methylcarbamoyl]-1-methyl-2-[2-[(5-methyl-1,3,4-oxadiazole-2-carbonyl)amino]propan-2-yl]-6-oxopyrimidin-5-olate. A two-dimensional molecular structure diagram of the anion is shown in Figure 1.

The presence of high-quality reference powder patterns in the Powder Diffraction File (PDF®; ICDD, 2014) is important for phase identification, particularly by pharmaceutical, forensic, and law enforcement scientists. The crystal structures of a significant fraction of the largest dollar volume pharmaceuticals have not been published, and thus calculated powder patterns are not present in the PDF-4 databases. Sometimes experimental patterns are reported, but they are generally of low quality. This structure is a result of a collaboration among ICDD, Illinois Institute of Technology, Poly Crystallography Inc., and Argonne National Laboratory to measure high-quality synchrotron powder patterns of commercial pharmaceutical ingredients, include these reference patterns in the PDF, and determine the crystal structures of these active pharmaceutical ingredients (APIs).

Even when the crystal structure of an API is reported, the single-crystal structure was often determined at low temperature. Most powder measurements are performed at ambient conditions. Thermal expansion (often anisotropic) means that the peak positions calculated from a low-temperature single-crystal structure often differ significantly from those measured at ambient conditions. These peak shifts can result

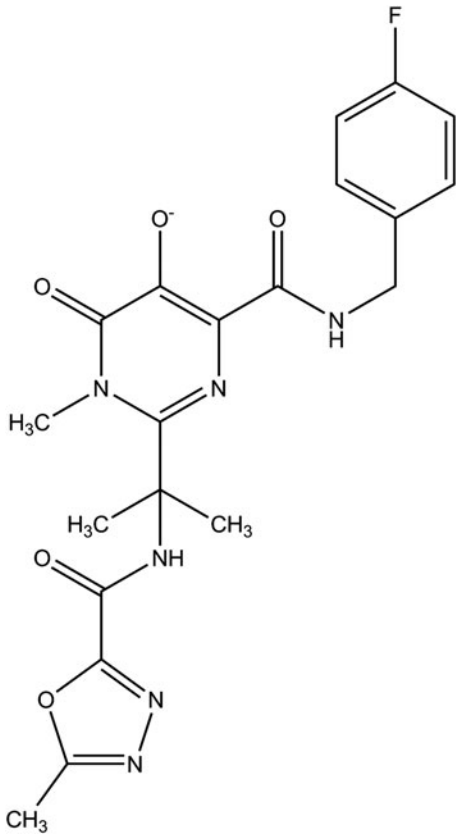

Figure 1. The molecular structure of the raltegravir anion.

[a]Author to whom correspondence should be addressed. Electronic mail: kaduk@polycrystallography.com

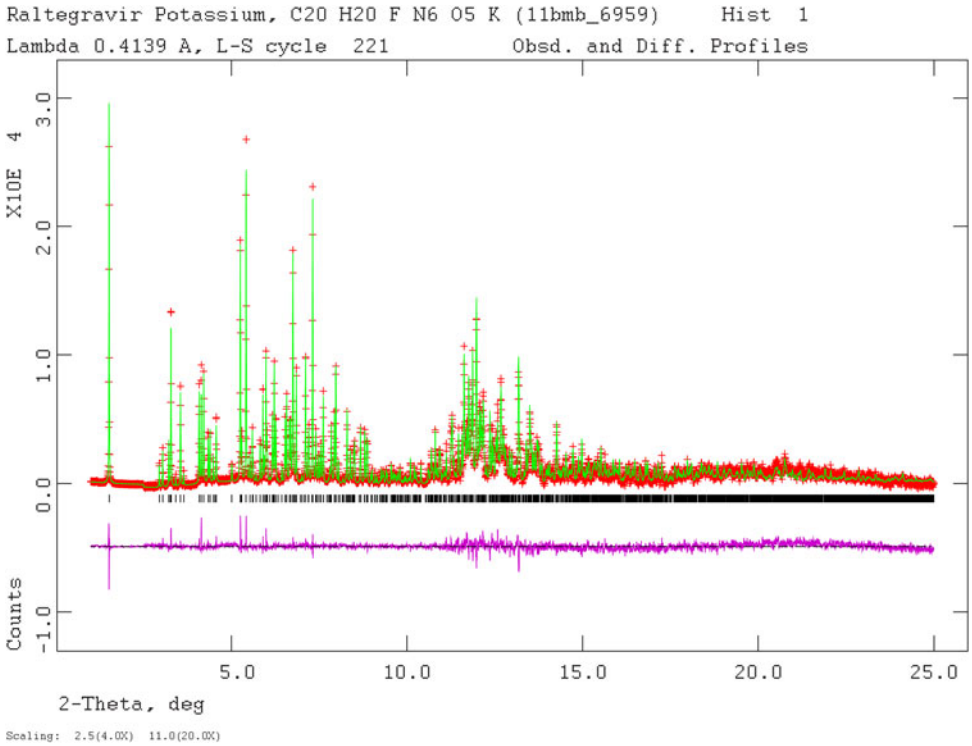

Figure 2. (Colour online) The Rietveld plot for the refinement of raltegravir potassium. The red crosses represent the observed data points, and the green line is the calculated pattern. The magenta curve is the difference pattern, plotted at the same vertical scales as the other patterns. The vertical scale has been multiplied by a factor of 4 for $2\theta > 2.5°$ and by a factor of 20 for $2\theta > 11.0°$.

TABLE I. Rietveld-refined crystal structure of raltegravir potassium.

Crystal data	
	$\beta = 94.1848(5)°$
Mw = 482.51	$V = 2045.72(1)$ Å^3
Monoclinic, $P2_1/c$	$Z = 4$
$a = 15.610\,59(9)$ Å	Synchrotron radiation, $\lambda = 0.413\,906$ Å
$b = 8.148\,19(3)$ Å	$T = 295$ K
$c = 16.125\,97(6)$ Å	Cylinder, 1.5 mm diameter
Data collection	
11-BM APS diffractometer	Scan method: step
Specimen mounting: Kapton capillary	$2\theta_{min} = 0.5°$, $2\theta_{max} = 50°$, $2\theta_{step} = 0.001°$
Data collection mode: transmission	
Refinement	
Least-squares matrix: full	23 999 data points
Rp = 0.061	Profile function: CW profile function number 4 with 21 terms. Pseudovoigt profile coefficients as parameterized in Thompson *et al.* (1987). Asymmetry correction of Finger *et al.* (1994). Microstrain broadening by Stephens (1999). #1(GU) = 4.786 #2(GV) = −0.126 #3(GW) = 0.063 #4(GP) = 0.000 #5(LX) = 0.727 #6(ptec) = 0.00 #7(trns) = 0.00 #8(shft) = 0.0000 #9(sfec) = 0.00 #10(S/L) = 0.0011 #11(H/L) = 0.0011 #12(eta) = 0.7911 #13(S400) = 5.5×10^{-3} #14(S040) = 3.1×10^{-2} #15(S004) = 6.4×10^{-4} #16(S220) = 1.6×10^{-2} #17(S202) = 8.9×10^{-4} #18(S022) = 7.1×10^{-4} #19(S301) = -2.3×10^{-3} #20(S103) = 3.5×10^{-5} #21(S121) = -4.4×10^{-3} Peak tails are ignored where the intensity is below 0.0020 times the peak Aniso. Broadening axis 0.0 0.0 1.0
$R_{wp} = 0.074$	121 parameters
$R_{exp} = 0.059$	71 restraints
$R(F^2) = 0.116\,10$	$(\Delta/\sigma)_{max} = 0.04$
$\chi^2 = 1.690$	Background function: GSAS background function number 1 with three terms. Shifted Chebyshev function of first kind 1: 151.8672: −36.71653: 16.8773

Continued

https://doi.org/10.1017/S0885715615000470 Published online by Cambridge University Press

TABLE I. Continued

Fractional atomic coordinates and isotropic displacement parameters (Å^2)

	x	*y*	*z*	U_{iso}
C1	0.0214 (2)	0.2598 (6)	0.5221 (3)	0.0705 (12)
C2	0.0935 (3)	0.2138 (4)	0.4817 (2)	0.0705 (12)
C3	0.1721 (2)	0.2900 (6)	0.5018 (3)	0.0705 (12)
C4	0.1786 (2)	0.4122 (5)	0.5623 (3)	0.0705 (12)
C5	0.1065 (3)	0.4581 (4)	0.6026 (2)	0.0705 (12)
C6	0.0279 (2)	0.3819 (6)	0.5825 (3)	0.0705 (12)
H7	0.0891 (5)	0.1295 (6)	0.4400 (3)	0.0826 (15)
H8	0.2218 (3)	0.2583 (9)	0.4740 (4)	0.0826 (15)
H9	0.1109 (5)	0.5424 (6)	0.6443 (3)	0.0826 (15)
H10	−0.0218 (3)	0.4136 (9)	0.6103 (4)	0.0826 (15)
F11	−0.0555 (3)	0.1912 (5)	0.5012 (3)	0.0705 (12)
C12	0.2648 (4)	0.4833 (7)	0.5907 (4)	0.0178 (10)
N13	0.3364 (3)	0.4239 (6)	0.5484 (3)	0.0178 (10)
C14	0.4103 (4)	0.3928 (8)	0.5915 (3)	0.0178 (10)
O15	0.4246 (3)	0.4343 (5)	0.6673 (2)	0.0178 (10)
C16	0.4797 (3)	0.3025 (7)	0.5508 (3)	0.0149 (6)
N17	0.5493 (3)	0.2643 (6)	0.6006 (2)	0.0149 (6)
C18	0.6147 (3)	0.1861 (7)	0.5699 (3)	0.0149 (6)
N19	0.6104 (3)	0.1340 (6)	0.4866 (2)	0.0149 (6)
C20	0.5387 (3)	0.1579 (8)	0.4353 (3)	0.0149 (6)
C21	0.4670 (3)	0.2405 (8)	0.4671 (3)	0.0149 (6)
O22	0.5328 (3)	0.1045 (5)	0.3623 (2)	0.0149 (6)
O23	0.3964 (3)	0.2677 (5)	0.4175 (2)	0.0149 (6)
C24	0.6812 (4)	0.0368 (7)	0.4544 (3)	0.0149 (6)
C25	0.6962 (3)	0.1758 (6)	0.6294 (3)	0.0308 (10)
C26	0.6783 (4)	0.2309 (7)	0.7146 (4)	0.0308 (10)
C27	0.7695 (4)	0.2787 (7)	0.5981 (4)	0.0308 (10)
N28	0.7202 (3)	−0.0009 (6)	0.6343 (3)	0.0308 (10)
C29	0.7886 (4)	−0.0574 (7)	0.6786 (4)	0.0308 (10)
O30	0.8580 (3)	0.0379 (5)	0.6966 (3)	0.0308 (10)
C31	0.8006 (4)	−0.2249 (7)	0.7151 (5)	0.0579 (12)
N32	0.7389 (3)	−0.3066 (7)	0.7459 (4)	0.0579 (12)
N33	0.7820 (4)	−0.4456 (6)	0.7850 (4)	0.0579 (12)
C34	0.8615 (3)	−0.4242 (8)	0.7689 (5)	0.0579 (12)
O35	0.8805 (3)	−0.2885 (6)	0.7282 (3)	0.0579 (12)
C36	0.9346 (5)	−0.5427 (8)	0.7986 (4)	0.0579 (12)
H37	0.256 89	0.617 93	0.574 46	0.0232 (14)
H38	0.277 69	0.4757	0.654 89	0.0232 (14)
H39	0.333 99	0.380 05	0.488 66	0.0232 (14)
H40	0.654 87	−0.077 22	0.427 02	0.0194 (8)
H41	0.700 68	0.107 99	0.396 61	0.0194 (8)
H42	0.732 75	0.019 55	0.4954	0.0194 (8)
H43	0.647 78	0.344 01	0.716 36	0.0400 (13)
H44	0.632 67	0.136 66	0.7458	0.0400 (13)
H45	0.736 39	0.226 11	0.755 52	0.0400 (13)
H46	0.735 94	0.397 49	0.584 03	0.0400 (13)
H47	0.817 89	0.290 94	0.643 89	0.0400 (13)
H48	0.790 71	0.230 43	0.540 97	0.0400 (13)
H49	0.674 43	−0.098 37	0.627 45	0.0753 (16)
H50	0.921 95	−0.592 03	0.859 43	0.0753 (16)
H51	0.973 74	−0.577 23	0.740 69	0.0753 (16)
H52	0.924 47	−0.667 46	0.757 05	0.0753 (16)
K53	0.452 33(14)	0.1455 (2)	0.760 49 (11)	0.0411 (7)

in failure of default search/match algorithms to identify a phase, even when it is present in the sample. High-quality reference patterns measured at ambient conditions are thus critical for easy identification of APIs using standard powder diffraction practices.

II. EXPERIMENTAL

Raltegravir potassium, a commercial reagent purchased from Jalor-Chem Co. Ltd., was used as-received. The white powder was packed into a 1.5 mm diameter Kapton capillary, and rotated during the measurement at ~50 cycles s^{-1}. The powder pattern was measured at 295 K at beam line 11-BM (Lee *et al.*, 2008; Wang *et al.*, 2008) of the Advanced Photon Source at Argonne National Laboratory using a wavelength of 0.413 906 Å from 0.5° to 50° 2θ with a step size of 0.001° and a counting time of 0.1 s/step. The pattern was indexed on a primitive monoclinic unit cell having $a = 15.6156$, $b = 8.1485$, $c = 16.1334$ Å, $\beta = 94.165°$, $V = 2047.44$ Å^3, and $Z = 4$ using DICVOL06 (Louër and Boultif,

https://doi.org/10.1017/S0885715615000470 Published online by Cambridge University Press

TABLE II. DFT-optimized (CRYSTAL09) crystal structure of raltegravir potassium. The lattice parameters were fixed at the experimental values.

Crystal data

$C_{20}H_{20}FKN_6O_5$
$Mw = 482.51$
Monoclinic, $P2_1/c$
$a = 15.610\ 59$ Å
$b = 8.148\ 19$ Å
$c = 16.125\ 97$ Å
$\beta = 94.1844°$
$V = 2045.72$ Å^3
$Z = 4$

Fractional atomic coordinates and isotropic displacement parameters (Å^2)

	x	*y*	*z*	U_{iso}*/*U*eq
C1	0.018 82	0.260 82	0.522 99	0.0705
C2	0.088 50	0.207 92	0.481 86	0.0705
C3	0.168 21	0.281 14	0.502 58	0.0705
C4	0.177 83	0.403 32	0.563 31	0.0705
C5	0.105 26	0.452 40	0.603 44	0.0705
C6	0.025 10	0.381 67	0.583 70	0.0705
H7	0.080 30	0.111 86	0.435 58	0.0826
H8	0.223 47	0.238 80	0.471 84	0.0826
H9	0.111 89	0.544 63	0.651 94	0.0826
H10	−0.031 52	0.422 62	0.612 82	0.0826
F11	−0.062 52	0.191 24	0.501 90	0.0705
C12	0.263 06	0.486 22	0.587 89	0.0178
N13	0.335 88	0.417 15	0.549 41	0.0178
C14	0.411 59	0.388 35	0.593 60	0.0178
O15	0.425 51	0.432 37	0.667 64	0.0178
C16	0.476 66	0.295 31	0.549 72	0.0149
N17	0.549 45	0.259 37	0.598 85	0.0149
C18	0.612 95	0.180 74	0.570 55	0.0149
N19	0.610 35	0.129 68	0.487 58	0.0149
C20	0.538 28	0.156 99	0.433 22	0.0149
C21	0.464 63	0.245 18	0.466 48	0.0149
O22	0.536 83	0.109 45	0.359 85	0.0149
O23	0.397 15	0.268 38	0.416 89	0.0149
C24	0.679 60	0.040 63	0.449 84	0.0149
C25	0.694 69	0.165 05	0.629 83	0.0308
C26	0.675 72	0.222 00	0.717 52	0.0308
C27	0.764 66	0.277 19	0.597 14	0.0308
N28	0.721 75	−0.010 33	0.638 41	0.0308
C29	0.796 10	−0.055 14	0.679 91	0.0308
O30	0.859 31	0.033 62	0.696 70	0.0308
C31	0.799 34	−0.227 83	0.712 18	0.0579
N32	0.738 70	−0.312 80	0.742 78	0.0579
N33	0.777 91	−0.450 21	0.779 76	0.0579
C34	0.859 38	−0.439 22	0.768 61	0.0579
O35	0.877 41	−0.300 38	0.726 19	0.0579
C36	0.929 08	−0.555 91	0.795 04	0.0579
H37	0.256 89	0.617 93	0.574 46	0.0232
H38	0.277 69	0.475 70	0.654 89	0.0232
H39	0.333 99	0.380 05	0.488 66	0.0232
H40	0.654 87	−0.077 22	0.427 02	0.0194
H41	0.700 68	0.107 99	0.396 61	0.0194
H42	0.732 75	0.019 55	0.495 40	0.0194
H43	0.647 78	0.344 01	0.716 36	0.0400
H44	0.632 67	0.136 66	0.745 80	0.0400
H45	0.736 39	0.226 11	0.755 52	0.0400
H46	0.735 94	0.397 49	0.584 03	0.0400
H47	0.817 89	0.290 94	0.643 89	0.0400
H48	0.790 71	0.230 43	0.540 97	0.0400
H49	0.674 43	−0.098 37	0.627 45	0.0753
H50	0.993 97	−0.497 21	0.785 73	0.0753
H51	0.921 65	−0.672 59	0.756 16	0.0753
H52	0.925 17	−0.587 59	0.863 51	0.0753
K53	0.452 25	0.150 86	0.760 67	0.0411

2007). The space group was indicated to be $P2_1/c$ by EXPO2009 (Altomare *et al.*, 2009). A search of this cell in the Cambridge Structural Database (Allen, 2002) yielded 85 hits, but no crystal structure for raltegravir potassium.

A raltegravir anion was built and its conformation optimized using Spartan'14 (Wavefunction, 2013), and saved as a mol2 file. This file was converted into a Fenske–Hall *Z*-matrix file using OpenBabel (O'Boyle *et al.*, 2011). Initial

https://doi.org/10.1017/S0885715615000470 Published online by Cambridge University Press

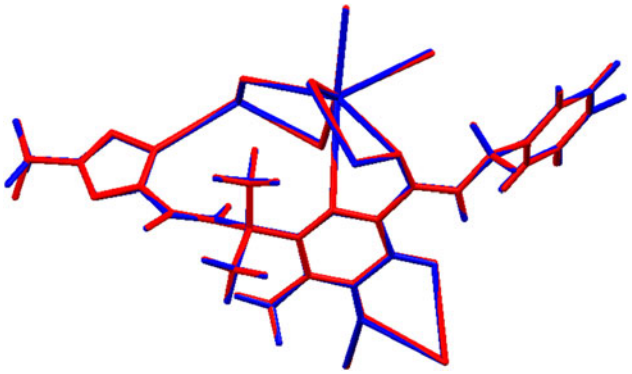

Figure 3. (Colour online) Comparison of the refined and optimized structures of raltegravir potassium. The Rietveld-refined structure is colored red and the DFT-optimized structure is in blue.

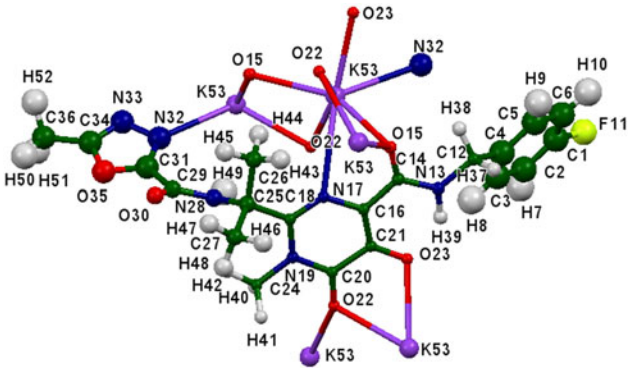

Figure 4. (Colour online) The molecular structure of raltegravir potassium, with the atom numbering. The atoms are represented by 50% probability spheroids.

attempts to solve the structure by simulated annealing techniques using this molecule and a potassium atom failed. Since the potassium cation would almost certainly be coordinated to the ionized hydroxyl oxygen, a potassium was added to O23 at a distance of 2.64 Å, and the geometry of the complex was optimized in Spartan '14 using molecular mechanics techniques. The hydrogen atoms were removed, and the molecule was saved as a .mol2 file. This file was converted into a MOPAC-format file using OpenBabel. This converted file was used to solve the structure using the simulated annealing module of EXPO2013 (Altomare *et al.*, 2013).

Rietveld refinement was carried out using General Structure Analysis System (GSAS) (Larson and Von Dreele, 2004). Only the 1°–25° portion of the pattern was included in the refinement. The C1–H10 phenyl group was refined as a rigid body. All other non-H bond distances and angles were subjected to restraints, based on a Mercury/Mogul Geometry Check (Bruno *et al.*, 2004; Sykes *et al.*, 2011) of the molecule. The Mogul average and standard deviation for each quantity were used as the restraint parameters. The restraints contributed 5.21% to the final χ^2. Isotropic displacement coefficients were refined, grouped by chemical similarity. The hydrogen atoms were included in calculated positions, which were recalculated during the refinement (Materials Studio; Accelrys, 2013). The U_{iso} of each hydrogen atom was constrained to be 1.3 × that of the heavy atom to which it is attached. The peak profiles were described using profile function #4 (Thompson *et al.*, 1987; Finger *et al.*, 1994), which includes the Stephens (1999) anisotropic strain broadening model. The background was modeled using a three-term shifted Chebyshev polynomial and a five-term diffuse scattering (Debye) function, to model the scattering from the Kapton capillary and any amorphous component of the sample. The final refinement of 121 variables using 24 070 observations (23 999 data points and 71 restraints) yielded the residuals $R_{wp} = 0.074$, $R_p = 0.061$, and $\chi^2 = 1.690$. The largest peak (0.45 Å from N17) and hole (1.95 Å from C18) in the difference Fourier map were 0.64 and −0.73 *e* Å−3, respectively. The Rietveld plot is included as Figure 2. The largest errors are in the shapes and intensities of a few low-angle peaks.

A density functional geometry optimization (fixed experimental unit cell) was carried out using CRYSTAL09 (Dovesi *et al.*, 2005). The basis sets for the H, C, N, and O atoms were those of Gatti *et al.* (1994), the basis set for F was that of Nada *et al.* (1993), and the basis set for K was that of Dovesi *et al.* (1993). The calculation used eight *k*-points and the B3LYP functional.

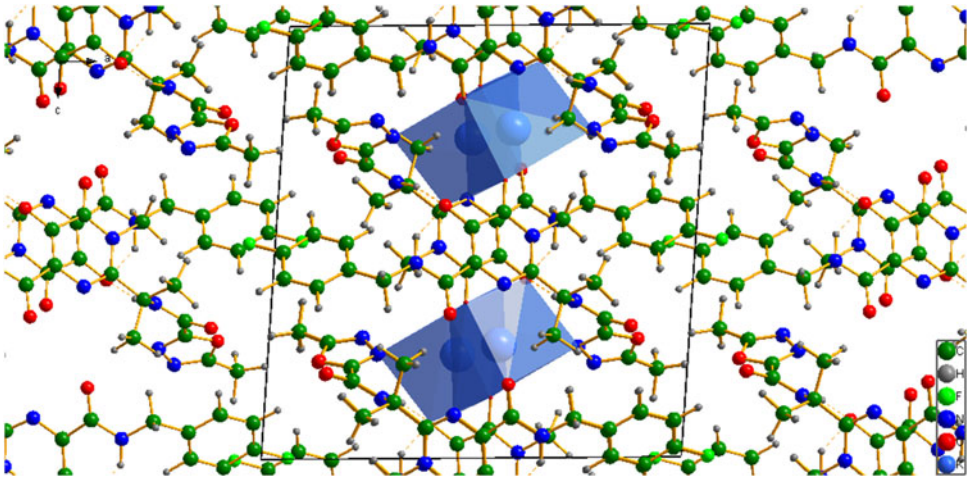

Figure 5. (Colour online) The crystal structure of raltegravir potassium, viewed down the *b*-axis.

https://doi.org/10.1017/S0885715615000470 Published online by Cambridge University Press

TABLE III. Unusual geometrical features in raltegravir potassium.

Quantity	Z-score	Optimized	Average
Bonds			
C18–N19	3.94	1.399	1.334 (17)
C16–N17	3.25	1.369	1.329 (12)
Angles			
C24–N19–C18	4.08	124.88	119.79 (125)
C16–C21–C20	4.00	115.62	120.10 (112)
C24–N19–C20	3.95	113.76	117.34 (91)
O23–C21–C16	3.64	126.67	123.40 (90)
O30–C29–C31	3.21	117.79	120.87 (96)
C16–N14–N13	3.16	115.96	120.47 (143)
Torsions			
C18–C25–N28–C29		173.1	
C26–C25–C18–N17		10.3	
C27–C25–C18–N17		−108.4	
N28–C25–C18–N17		127.0	
N28–C25–C18–N19		−60.0	
N32–C31–C29–C28		−36.9	

III. RESULTS AND DISCUSSION

The refined atom coordinates of raltegravir potassium are reported in Table I, and the coordinates from the density functional theory (DFT) optimization in Table II. The root-mean-square deviation of the non-hydrogen atoms is 0.06 Å, and the maximum deviation is 0.16 Å, at the methyl group C36 (Figure 3). The excellent agreement between the refined and optimized structures is strong evidence that the structure is correct (van de Streek and Neumann, 2014). The discussion of the geometry uses the DFT-optimized structure. The asymmetric unit (with atom numbering) is illustrated in Figure 4, and the crystal structure is presented in Figure 5.

Most bond distances, angles, and torsion angles fall within the normal ranges indicated by a Mercury Mogul Geometry Check, but several geometrical features are flagged as unusual (Table III). Many of these occur in the C_4N_2 ring C16–C21 in the center of the molecule; this ring is also close to the K coordination. Several unusual torsion angles occur in the C25–C31 portion of the molecule, but there are only a few comparison angles. Apparently, the geometry of this molecule is somewhat unusual.

The most prominent feature of the crystal structure is the chains of edge-sharing 7-coordinate K parallel to the *b*-axis. The coordination is KO_5N_2, and the K–N bonds are the longest, as expected from the bond valence r_0 (2.13 and 2.26 Å for K–O and K–N, respectively) (Breese and O'Keefe, 1991). The raltegravir molecule chelates to the K through N17 and O15. The bond valence sum for the K is 1.01. The Mulliken overlap populations are small and positive (<0.008 *e*), suggesting that the K–O/N bonds have a small degree of covalent character, but are mainly ionic.

Conformational analysis of the raltegravir anion (Hartree–Fock/3-21G/water) suggests that the solid-state conformation is at least 22 kcal mole^{-1} higher in energy than the minimum-energy conformation, and that K coordination and the hydrogen bonds contribute significantly to the observed structure. An analysis of the contributions to the total crystal energy using the Forcite module of Materials Studio (Accelrys, 2013) suggests that significant contributions to the crystal energy come from bond, angle, and torsion distortion terms. The crystal energy appears to be dominated by electrostatic contributions, which in this force-field-based analysis include hydrogen bonds. The hydrogen bonds are better analyzed using the results of the DFT calculation.

The carbonyl oxygen O23 participates in two strong hydrogen bonds (Table IV). The N13–H39···O23 bond is intermolecular. The graph sets (Etter, 1990; Bernstein *et al.*, 1995; Shields *et al.*, 2000) are S1,1(6) and R1,1(7), hydrogen bonds, respectively; the seven-membered ring includes the K. Several weak C–H···O/F hydrogen bonds (both intra- and inter-molecular) apparently help determine the conformation of the raltegravir anion in the solid state. The crystal structure can be described as having K-containing layers in the *bc*-plane, with double layers of CH_4F phenyl rings halfway between them.

The Bravais–Friedel–Donnay–Harker (Bravais, 1866; Friedel, 1907; Donnay and Harker, 1937) morphology suggests that we might expect platy morphology for raltegravir potassium, with {100} as the principal faces. A second-order spherical harmonic preferred orientation model was included in the refinement, but the texture index was only 1.002; preferred orientation was not significant for this rotated capillary specimen. The powder pattern of raltegravir potassium is included in the PDF as entry 00-064-1499.

ACKNOWLEDGMENTS

Use of the Advanced Photon Source at Argonne National Laboratory was supported by the U.S. Department of Energy, Office of Science, Office of Basic Energy Sciences, under Contract No. DE-AC02-06CH11357. This work was partially supported by the International Centre for Diffraction Data. The authors thank Lynn Ribaud for his assistance in data collection and Corrado Cuocci for his help in using the simulated annealing module of EXPO2013.

TABLE IV. Hydrogen bonds in raltegravir potassium.

D–H···A	D–H (Å)	H···A (Å)	D···A (Å)	D–H···A (°)	Overlap (*e*)
N13–H39···O23	1.024	1.818	2.692	141.1	0.067
N28–H49···O23	1.036	1.887	2.902	165.5	0.068
C12–H38···O15	1.091	2.393	2.793	103.5	0.014
C24–H40···O22	1.089	2.567	2.63	81.1	0.005
C36–H51···O30	1.091	2.328	3.376	160.6	0.021
C27–H47···O30	1.086	2.336	2.89	109.7	0.006
C36–H50···F11	1.093	2.432	3.507	169.2	0.009

https://doi.org/10.1017/S0885715615000470 Published online by Cambridge University Press

Accelrys (**2013**). *Materials Studio 7.0* (Accelrys Software Inc., San Diego, CA).

Allen, F. H. (**2002**). "The Cambridge Structural Database: a quarter of a million crystal structures and rising," Acta Crystallogr. B, Struct. Sci. **58**, 380–388.

Altomare, A., Camalli, M., Cuocci, C., Giacovazzo, C., Moliterni, A., and Rizzi, R. (**2009**). "EXPO2009: structure solution by powder data in direct and reciprocal space," J. Appl. Crystallogr. **42**(6), 1197–1202.

Altomare, A., Cuocci, C., Giacovazzo, C., Moliterni, A., Rizzi, R., Corriero, N., and Falcicchio, A. (**2013**). "EXPO2013: a kit of tools for phasing crystal structures from powder data", J. Appl. Crystallogr. **46**, 1231–1235.

Bernstein, J., Davis, R. E., Shimoni, L., and Chang, N. L. (**1995**). "Patterns in hydrogen bonding: functionality and graph set analysis in crystals," Angew. Chem., Int. Ed. Engl. **34**(15), 1555–1573.

Bravais, A. (**1866**). *Etudes Cristallographiques* (Gauthier Villars, Paris).

Breese, N. E. and O'Keefe, M. (**1991**). "Bond-valence parameters for solids," Acta Crystallogr. B **47**, 192–197.

Bruno, I. J., Cole, J. C., Kessler, M., Luo, J., Motherwell, W. D. S., Purkis, L. H., Smith, B. R., Taylor, R., Cooper, R. I., Harris, S. E., and Orpen, A. G. (**2004**). "Retrieval of crystallographically-derived molecular geometry information," J. Chem. Inf. Sci. **44**, 2133–2144.

Croxtall, J. D. and Keam, S. J. (**2009**). "Raltegravir," Drugs **69**(8), 1059–75.

Donnay, J. D. H. and Harker, D. (**1937**). "A new law of crystal morphology extending the law of Bravais," Am. Mineral. **22**, 446–467.

Dovesi, R., Roetti, C., Freyria Fava, C., Prencipe, M., and Saunders, V. R. (**1993**). "On the elastic properties of lithium, sodium, and potassium oxide. An *ab initio* study," Chem. Phys. **156**, 11–19.

Dovesi, R., Orlando, R., Civalleri, B., Roetti, C., Saunders, V. R., and Zicovich-Wilson, C. M. (**2005**). "CRYSTAL: a computational tool for the *ab initio* study of the electronic properties of crystals," Z. Kristallogr. **220**, 571–573.

Etter, M. C. (**1990**). "Encoding and decoding hydrogen-bond patterns of organic compounds," Acc. Chem. Res. **23**(4), 120–126.

Finger, L. W., Cox, D. E., and Jephcoat, A. P. (**1994**). "A correction for powder diffraction peak asymmetry due to axial divergence," J. Appl. Crystallogr. **27**(6), 892–900.

Friedel, G. (**1907**). "Etudes sur la loi de Bravais," Bull. Soc. Fr. Mineral. **30**, 326–455.

Gatti, C., Saunders, V. R., and Roetti, C. (**1994**). "Crystal-field effects on the topological properties of the electron-density in molecular crystals – the case of urea," J. Chem. Phys. **101**, 10686–10696.

ICDD (**2014**). *PDF-4+ 2014 (Database)*, edited by S. Kabekkodu (International Centre for Diffraction Data, Newtown Square, PA).

Jetti, R. R., Jonnalagadda, M., Raval, C. K., and Datta, D. (**2011**). Novel polymorphs of raltegravir, WO 2011024192 A2.

Larson, A. C. and Von Dreele, R. B. (**2004**). *General Structure Analysis System (GSAS)* (Report LAUR 86–784). Los Alamos, New Mexico: Los Alamos National Laboratory.

Lee, P. L., Shu, D., Ramanathan, M., Preissner, C., Wang, J., Beno, M. A., Von Dreele, R. B., Ribaud, L., Kurtz, C., Antao, S. M., Jiao, X., and Toby, B. H. (**2008**). "A twelve-analyzer detector system for high-resolution powder diffraction," J. Synchrotron Radiat. **15**(5), 427–432.

Louër, D. and Boultif, A. (**2007**). "Powder pattern indexing and the dichotomy algorithm," Z. Kristallogr. Suppl. 191–196.

Nada, R., Catlow, C. R. A., Pisani, C., and Orlando, R. (**1993**). "*Ab initio* Hartree–Fock perturbed-cluster study of neutral defects in LiF," Model. Simul. Mater. Sci. Eng. **1**, 165–187.

O'Boyle, N., Banck, M., James, C. A., Morley, C., Vandermeersch, T., and Hutchison, G. R. (**2011**). "Open Babel: an open chemical toolbox," J. Chem. Inf., 1–14. doi:10.1186/1758-2946-3-33.

Parthasaradhi, R. B., Rathnakar, R. K., Raji, R. R., Muralidhara, R. D., and Subash, C. R. K. (**2010**). Novel polymorphs of raltegravir potassium, WO 2010140156 A2.

Shields, G. P., Raithby, P. R., Allen, F. H., and Motherwell, W. S. (**2000**). "The assignment and validation of metal oxidation states in the Cambridge Structural Database," Acta Crystallogr. B, Struct. Sci. **56**(3), 455–465.

Stephens, P. W. (**1999**). "Phenomenological model of anisotropic peak broadening in powder diffraction," J. Appl. Crystallogr. **32**, 281–289.

Sykes, R. A., McCabe, P., Allen, F. H., Battle, G. M., Bruno, I. J. and Wood, P. A. (**2011**). "New software for statistical analysis of Cambridge Structural Database data," J. Appl. Crystallogr. **44**, 882–886.

Thompson, P., Cox, D. E., and Hastings, J. B. (**1987**). "Rietveld refinement of Debye–Scherrer synchrotron X-ray data from Al_2O_3," J. Appl. Crystallogr. **20**(2), 79–83.

van de Streek, J. and Neumann, M. A. (**2014**). "Validation of molecular crystal structures from powder diffraction data with dispersion-corrected density functional theory (DFT-D)," Acta Crystallogr. B, Struct. Sci. **70**(6), 1020–1032.

Wang, J., Toby, B. H., Lee, P. L., Ribaud, L., Antao, S. M., Kurtz, C., Ramanathan, M., Von Dreele, R. B., and Beno, M. A. (**2008**). "A dedicated powder diffraction beamline at the advanced photon source: commissioning and early operational results," Rev. Sci. Instrum. **79**, 085105.

Wavefunction Inc. (**2013**). *Spartan'14 Version 1.1.0* (Wavefunction Inc., Irvine, California).